ORGANIC CHEMISTRY FRONTIERS

RESEARCH ARTICLE

View Article Online
View Journal | View Issue

Cite this: *Org. Chem. Front.*, 2024, **11**, 3214

Palladium-catalyzed and ligand-controlled divergent cycloadditions of vinylidenecyclopropane-diesters with *para*-quinone methides enabled by zwitterionic π-propargyl palladium species†

Jia-Hao Shen,[a] Yong-Jie Long,[b] Min Shi [b] and Yin Wei *[a,b]

Received 27th February 2024,
Accepted 14th April 2024

DOI: 10.1039/d4qo00368c

rsc.li/frontiers-organic

A palladium-catalyzed divergent synthesis of spiro-cyclohexadienones with a five- or a six-membered ring by a cycloaddition reaction of vinylidenecyclopropane-diesters (VDCP-diesters) with *p*-quinone methides (*p*-QMs) was disclosed. This protocol features a switchable process between [3 + 2] and [4 + 2] cycloadditions tuned by subtle choice of the phosphine ligand. The substrate scopes have been investigated and the reaction mechanism has been clarified by mechanistic studies; and DFT calculations also revealed that the coordination modes of the ligands with the substrates and the bite angle of the ligands play critical roles in the product regioselectivity.

Introduction

Spiro-cyclohexadienones are widely found as natural molecular backbones in bioactive natural products and have been important sources of medicines and organic synthetic building blocks (Fig. 1).[1] Thus, great efforts have been devoted to the synthesis of functionalized spiro-cyclohexadienones.[2] Several strategies for the efficient construction of spiro-cyclohexadienones have been reported in recent years.[3] The *p*-QM consists of a cyclohexadiene moiety that is in *para*-conjugation with a carbonyl group and an *exo*-methylene component, which serves as an important intercalated allylic Michael receptor.[1c,4] The ability of the *para* double bond to undergo nucleophilic addition with a wide range of nucleophilic reagents enables [2 + *n*] spirocyclization products to be provided.[5–7] Spirocyclopropanation reaction of *p*-QMs with α-keto carbonyls,[5d] carbocyclic spiro[5,5]undeca-1,4-dien-3-ones *via* 1,6-conjugate addition initiated formal [4 + 2] annulation sequences,[7a] and Pd-catalyzed annulated coupling of spirovinyl-cyclopropyl oxindoles with *p*-QMs (Scheme 1a) were reported in recent years.[3c] Very recently, the metal-free cycloaddition reactions of *p*-QMs with halo alcohols to generate divergent types of total carbon spiro-cyclohexadienone compounds were also reported.[7e]

On the other hand, cycloaddition reactions *via* amphiphilic palladium species have been intensely studied in the past few years,[8] wherein palladium-catalyzed reactions of propargyl species are challenging due to the greater complexity in achieving regioselective and chemoselective transformations.[9] In recent years, our group has developed and explored a series of reactions employing vinylidenecyclopropane (VDCP)

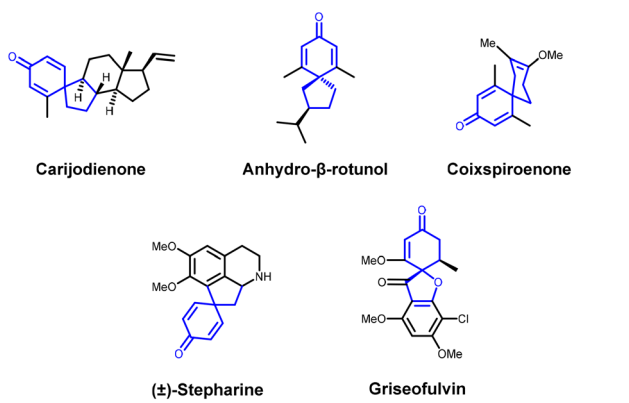

Fig. 1 Representative bioactive compounds bearing spiro-cyclohexadienone.

[a]*School of Materials and Chemistry, University of Shanghai for Science and Technology, 516 Jungong Road, Shanghai, 200093, China*
[b]*State Key Laboratory of Organometallic Chemistry, Center for Excellence in Molecular Synthesis, Shanghai Institute of Organic Chemistry, University of Chinese Academy of Sciences, Chinese Academy of Sciences, 345 Lingling Road, Shanghai 200032, China. E-mail: weiyin@sioc.ac.cn*

†Electronic supplementary information (ESI) available: Experimental procedures; characterization data for new compounds. CCDC 2225338 and 2288733. For ESI and crystallographic data in CIF or other electronic format see DOI: https://doi.org/10.1039/d4qo00368c

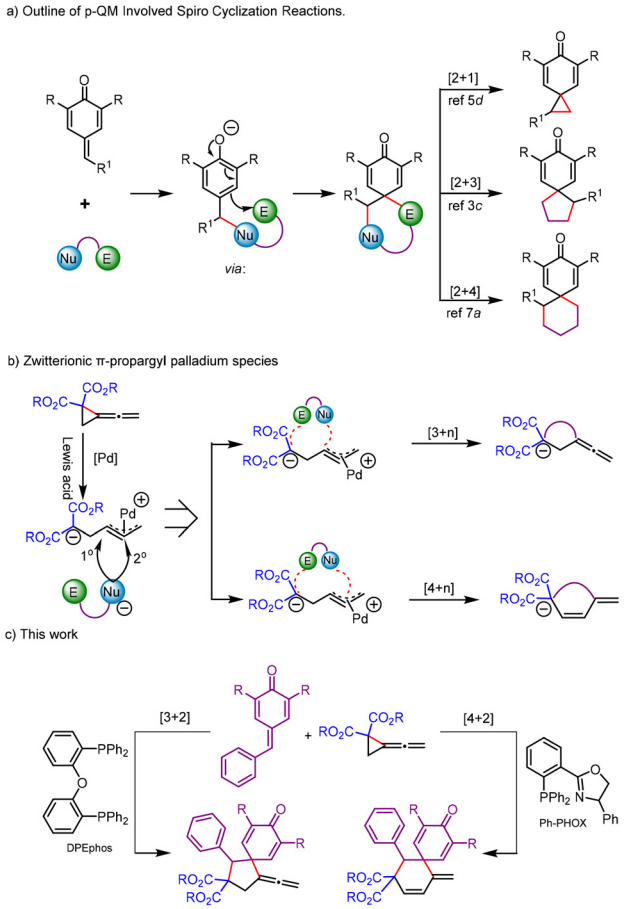

Scheme 1 Previous works and this work.

derivatives,[9b,10] which are small cyclic compounds containing a highly reactive cyclopropane ring attached to an allene moiety. In 2021, our group reported the first reaction of zwitterionic π-propargyl palladium species derived from VDCP-diesters,[11] which realized the regio-divergent synthesis of spirooxindoles fused with a five- or a six-membered ring by switching the phosphine ligand (Scheme 1b). The zwitterionic π-propargyl palladium species was proposed as the key reaction intermediate (Scheme 1b); however, the demonstration of the mechanism of the reaction was not revealed clearly in previous work.

Based on the previous research and the progress of our group's research on zwitterionic π-propargyl palladium species from vinylidenecyclopropane-diesters (VDCP-diesters),[11] we anticipated the palladium-catalyzed cycloaddition of *p*-QMs with VDCP-diesters to be an effective and facile method to provide a series of spiro-cyclohexadienone compounds. Herein, we wish to report the palladium-catalyzed cycloadditions of *p*-QMs with VDCP-diesters which were tuned by phosphorus ligands to generate diverse spiro-products, and explore the reaction mechanism involving the zwitterionic π-propargyl palladium species as the key reaction intermediates and critical factors influencing the cycloaddition modes (Scheme 1c).

To explore the proposed synthesis of spiro-cyclohexadienones, we started with a model reaction employing *p*-quinone methide **1a** and VDCP-diester **2a** as the substrates, and optimized the reaction conditions using Pd_2dba_3 as a palladium catalyst, DPEphos as a ligand, $Yb(OTf)_3$ as a Lewis acid additive, 4 Å MS as an additive and Cs_2CO_3 as an inorganic base additive in tetrahydrofuran (THF) at 65 °C for 22 h. Gratifyingly, the corresponding [3 + 2] spiro-cyclohexadienone product **3a** was obtained as a single product in a yield of 24% (Scheme S1 in the ESI†). The structure was unambiguously determined by X-ray diffraction. The ORTEP drawing is shown in Scheme 2 and the CIF data are summarized in the ESI.† First, we examined the temperature influence and determined that the optimal reaction temperature was 45 °C (Table 1, entries 1–4). To enhance the nucleophilicity of the substrate *p*-QMs, DMAP (50 mol%) was added into the reaction system, and we identified that the reaction produced **3a** in 68% yield under otherwise identical conditions (Table 1, entry 5). Then, we further examined the solvent effects, and using MeCN as the solvent, the desired product was obtained in 85% yield and that served as the optimal reaction condition. The use of other solvents, such as toluene, DCE, dioxane, DMF and DMSO, furnished the desired products in 27%–82% yields (Table 1, entries 6–11). Using Binap and Xantphos as ligands gave **3a** in lower yields (32% yield with Xantphos and 55% yield with Binap) than that using DPEphos (Table 1, entries 12 and 13). Moreover, we examined the base additives and found that using both organic and inorganic bases did not work as well as Cs_2CO_3 (Table 1, entries 14 and 15). Changing the palladium source from Pd_2dba_3 to $Pd(OAc)_2$ and $Pd(PPh_3)_4$ did not affect the yield significantly, giving **3a** in 77% and 79% yields, respectively (Table 1, entries 16 and 17).

Surprisingly, we obtained a mixture of [4 + 2] cycloaddition product **4a** and [3 + 2] cycloaddition product **3a** employing the Ph-PHOX ligand, during optimization of the phosphorous ligands. Next, we turned our attention to further optimizing the reaction conditions for generation of the [4 + 2] cycloaddition product **4a**. We also examined the reaction under similar conditions to those mentioned above. Temperature and solvents were primarily examined, and the yield of **4a** increased to 74% and the total yield was 97% when 1,4-dioxane was used as the solvent (Table 2, entry 3). In the case of using the DPEphos ligand, the total yield of products decreased with increasing reaction temperature. Overall, the optimal conditions for the production of **4a** were to carry out the reaction in 1,4-dioxane at 45 °C for 12 h with Ph-PHOX as a ligand. The X-ray crystal structure of **4a** is shown in Scheme 3.

On the basis of the above optimized conditions for this divergent cycloaddition reaction, the substrate scope for the [3 + 2] cycloaddition reactions between *p*-QMs **1** and the zwitterionic π-propargyl palladium species generated from VDCP-diesters **2** was investigated, and the results are shown in Scheme 2. Fixing the R^2 group as a *t*-butyl group, whether an electron-withdrawing or -donating substituent was introduced at the *para*-position of the benzene ring on the *p*-QM, the reac-

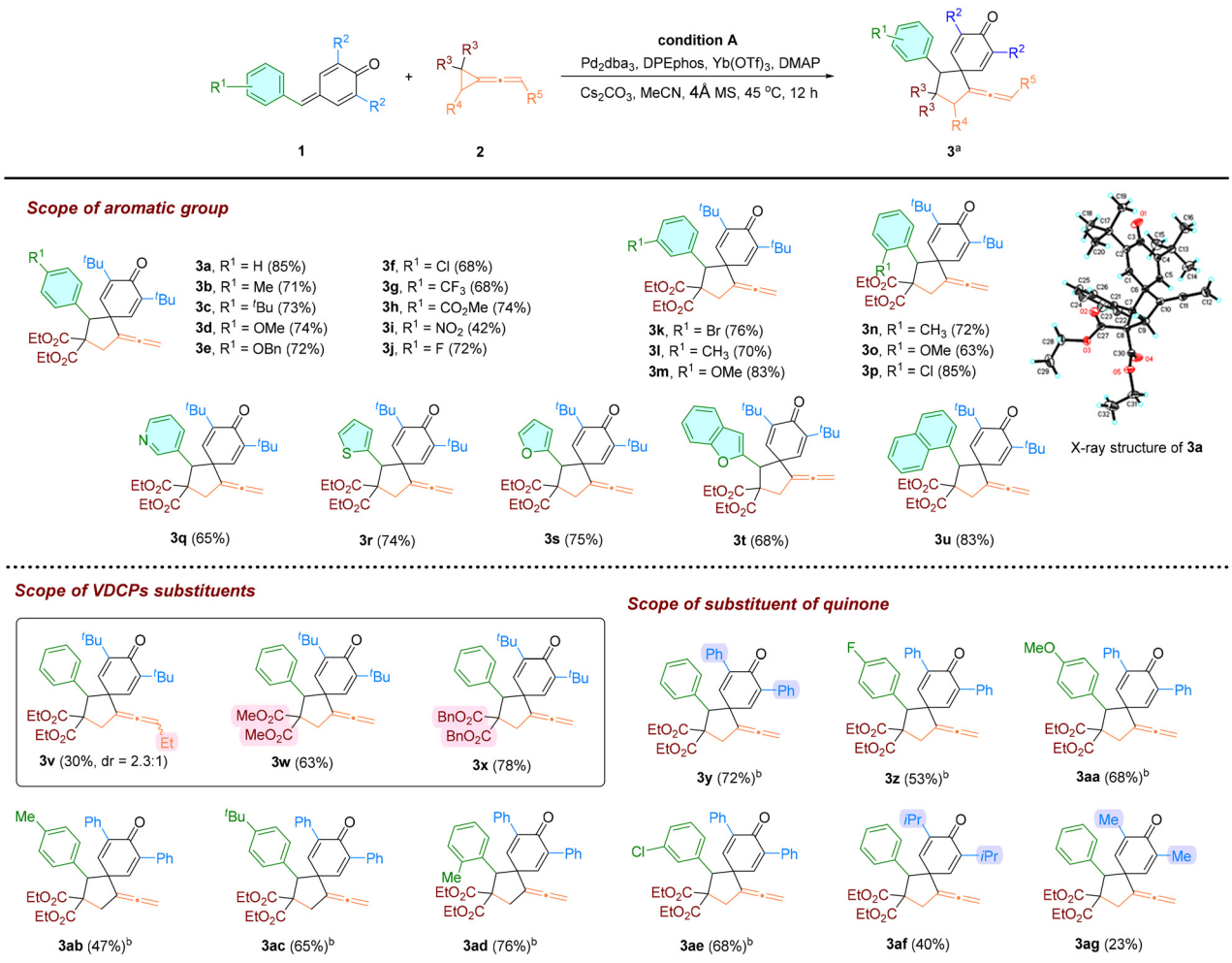

(a) Reaction conditions: a solution of **1** (0.1 mmol) and **2** (0.25 mmol), Pd_2dba_3 (2.5 mol%), DPEphos (7.5 mol%), $Yb(OTf)_3$ (10.0 mol%), 4Å MS (100 mg), DMAP (50.0 mol%) and Cs_2CO_3 (0.1 mmol) in MeCN (1.0 mL) was heated at 45 °C for 12 h, isolated yield. (b) DMF as solvent.

Scheme 2 Substrate scope of [3 + 2] cycloaddition between *p*-QMs **1** and VDCPs **2**. [a] Reaction conditions: a solution of **1** (0.1 mmol) and **2** (0.25 mmol), Pd_2dba_3 (2.5 mol%), DPEphos (7.5 mol%), $Yb(OTf)_3$ (10.0 mol%), 4 Å MS (100 mg), DMAP (50.0 mol%) and Cs_2CO_3 (0.1 mmol) in MeCN (1.5 mL) was heated at 45 °C for 12 h; isolated yield. [b] DMF as solvent.

tions proceeded smoothly, and the target products **3a–3j** were obtained in 42%–85% yields. The low yield of the nitro-substituted product **3i** was probably due to the low stability of the product. Employing substrates having substituents at the *meta*-position of the benzene ring, the target products **3k–3m** were also obtained in 70% to 83% yields. In addition, substrates **1n–1p** having substituents at the *ortho*-position of the benzene ring were tolerated in this reaction, affording the desired products **3n–3p** in 63% to 85% yields. R^1 groups that were a heterocycle or a fused aromatic ring also gave the desired products **3q–3u** in 65% to 83% yields. However, the reaction did not occur when R^1 was a methyl group; this result indicated that the aryl ring structure was necessary (Scheme S3 in the ESI†). In addition, we tested the reaction of substrate VDCP-diester **1v** having an ethyl group at the terminal position of the allene moiety, and the corresponding product **3v** was obtained in 30% yield with 2.3 : 1 dr, probably due to steric effects. Methyl- and benzyl-substituted VDCP were also reacted with *p*-QMs to produce the desired products, giving the desired products **3w** and **3x** in 63% and 78% yields, respectively. However, when the VDCP-diester had an isopropyl group at R^4, the corresponding product was not obtained (Scheme S3 in the ESI†). We then examined the R^2 group and found that when the *t*-butyl group was replaced with a phenyl group, the reaction proceeded smoothly with DMF as the solvent and the target product **3y** was obtained in 72% yield. Subsequently, keeping R^2 as a phenyl group, variation of R^1 produced **3z–3ae** in moderate yields under the same conditions. However, when the R^2 group was changed from *t*-butyl to isopropyl and methyl groups, a significant decrease in yield ensued, with **3af** and **3ag** produced in 40% and 23% yields, respectively.

Next, the scope of the [4 + 2] cycloaddition reaction was also investigated under the optimal conditions, and the results are displayed in Scheme 3. Note that the yields were deter-

Table 1 Optimization of reaction conditions for generation of product **3a**

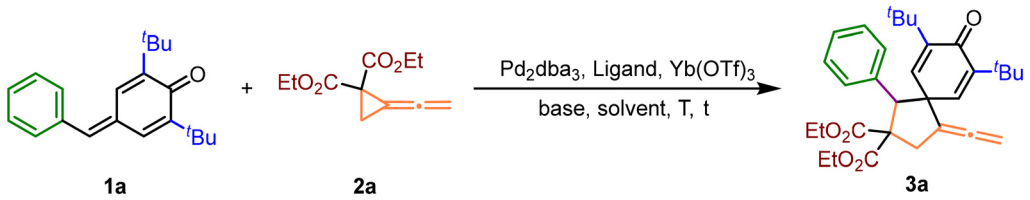

1a **2a** **3a**

Entry[a]	**2a** (equiv.)	[Pd]	Ligand	Solvent	Base	DMAP (mol%)	*T*, °C	*t* (h)	Yield[b] (%)
1	2.5	Pd_2dba_3	DPEphos	THF	Cs_2CO_3	—	40	22	29
2	2.5	Pd_2dba_3	DPEphos	THF	Cs_2CO_3	—	45	22	46
3	2.5	Pd_2dba_3	DPEphos	THF	Cs_2CO_3	—	50	22	36
4	2.5	Pd_2dba_3	DPEphos	THF	Cs_2CO_3	—	55	22	31
5	2.5	Pd_2dba_3	DPEphos	THF	Cs_2CO_3	50	45	12	68
6	2.5	Pd_2dba_3	DPEphos	Dioxane	Cs_2CO_3	50	45	12	45
7	**2.5**	**Pd_2dba_3**	**DPEphos**	**MeCN**	**Cs_2CO_3**	**50**	**45**	**12**	**85**
8	2.5	Pd_2dba_3	DPEphos	Toluene	Cs_2CO_3	50	45	12	27
9	2.5	Pd_2dba_3	DPEphos	DCE	Cs_2CO_3	50	45	12	44
10	2.5	Pd_2dba_3	DPEphos	DMF	Cs_2CO_3	50	45	12	57
11	2.5	Pd_2dba_3	DPEphos	DMSO	Cs_2CO_3	50	45	12	82
12	2.5	Pd_2dba_3	Binap	MeCN	Cs_2CO_3	50	45	12	55
13	2.5	Pd_2dba_3	Xantphos	MeCN	Cs_2CO_3	50	45	12	32
14	2.5	Pd_2dba_3	DPEphos	MeCN	DBU	50	45	12	54
15	2.5	Pd_2dba_3	DPEphos	MeCN	KH_2PO_4	50	45	12	Trace
16	2.5	$Pd(OAc)_2$	DPEphos	MeCN	Cs_2CO_3	50	45	12	77
17	2.5	$Pd(PPh_3)_4$	DPEphos	MeCN	Cs_2CO_3	50	45	12	79

[a] Reaction conditions: a solution of **1a** (0.1 mmol) and **2a** (0.25 mmol), [Pd] (5.0 mol%), ligand (7.5 mol%), 4 Å MS (100 mg), $Yb(OTf)_3$ (10.0 mol%) and base (0.1 mmol) in solvent (1.5 mL) was heated at 45 °C for 12 h. [b] Isolated yield.

Table 2 Optimization of reaction conditions for generation of product **4a**

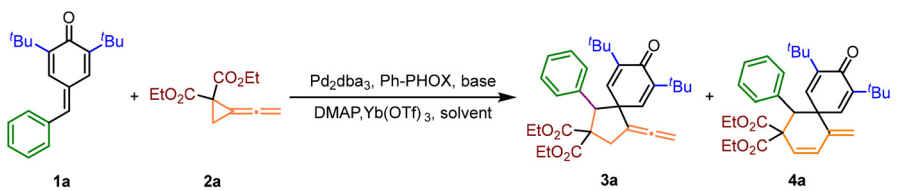

1a **2a** **3a** **4a**

Entry[a]	**2a** (equiv.)	Solvent	Base	*T* (°C)	*t* (h)	Total yield[b] (%)	**3a** : **4a**, yield[b] (%)
1	2.5	THF	Cs_2CO_3	45	12	84	21 : 63
2	2.5	MeCN	Cs_2CO_3	45	12	88	24 : 64
3	**2.5**	**1,4-Dioxane**	**Cs_2CO_3**	**45**	**12**	**97**	**23 : 74**
4	2.5	DMF	Cs_2CO_3	45	12	91	24 : 67
5	2.5	DCM	Cs_2CO_3	45	12	95	28 : 67
6	2.5	Toluene	Cs_2CO_3	45	12	91	35 : 56
7	2.5	DMSO	Cs_2CO_3	45	12	73	26 : 47
8	2.5	DCE	Cs_2CO_3	45	12	34	7 : 27
9	2.5	1,4-Dioxane	Cs_2CO_3	55	12	91	28 : 63
10	2.5	1,4-Dioxane	Cs_2CO_3	65	12	85	27 : 58

[a] Reaction conditions: a solution of **1a** (0.1 mmol) and **2a** (0.25 mmol), [Pd] (5.0 mol%), PH = PHOX (7.5 mol%), $Yb(OTf)_3$ (10.0 mol%), 4 Å MS (100 mg), DMAP (50 mol%) and base (0.1 mol) in solvent (1.5 mL) was heated at 45 °C for 12 h. [b] Yields were determined by ^1H NMR using dibromomethane as an internal standard.

mined by ^1H NMR using dibromomethane as an internal standard due to the difficulty of separating the reaction products. Substrates **1** bearing different substituents at the *para*- and *meta*-positions on the benzene ring could be converted to the corresponding products **4a–4i** in 49–74% yields. However, the yield was lower when the *ortho*-position was methyl substituted, with **4j** afforded in 37% yield, and **4k** and **4l** in which the same position had methoxy and chlorine substituents were obtained in 50% and 70% yields, respectively. Moreover, *p*-QMs containing fused aromatic rings and heterocycles were also tolerated in this reaction, affording the corresponding products **4m–4q** in 33% to 60% yields. In addition, on chan-

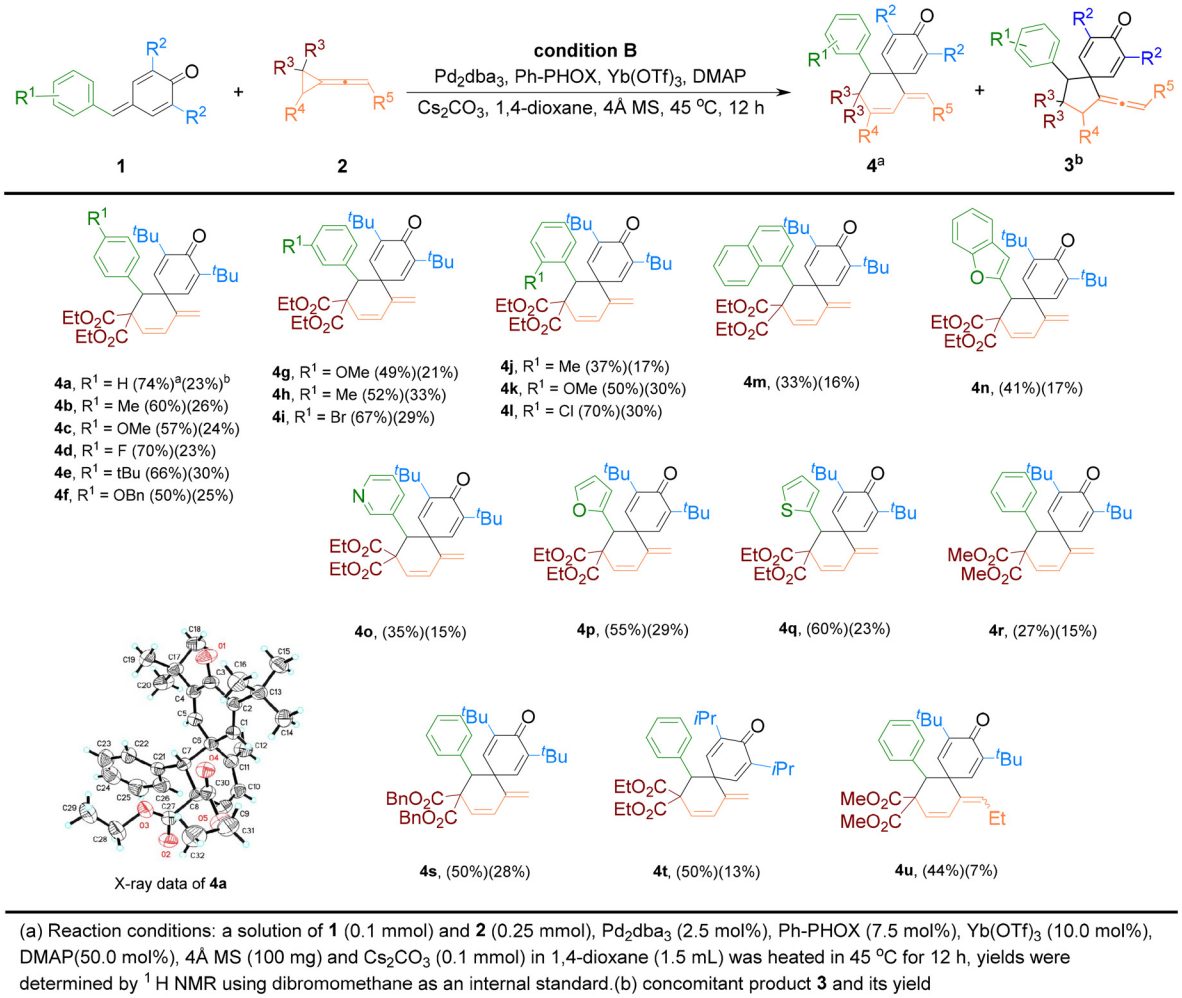

(a) Reaction conditions: a solution of **1** (0.1 mmol) and **2** (0.25 mmol), Pd_2dba_3 (2.5 mol%), Ph-PHOX (7.5 mol%), $Yb(OTf)_3$ (10.0 mol%), DMAP(50.0 mol%), 4Å MS (100 mg) and Cs_2CO_3 (0.1 mmol) in 1,4-dioxane (1.5 mL) was heated in 45 °C for 12 h, yields were determined by ^{1}H NMR using dibromomethane as an internal standard.(b) concomitant product **3** and its yield

Scheme 3 Substrate scope of [4 + 2] cycloaddition between *p*-QMs **1** and VDCPs **2**. [a] Reaction conditions: a solution of **1** (0.1 mmol) and **2** (0.25 mmol), Pd_2dba_3 (2.5 mol%), Ph-PHOX (7.5 mol%), $Yb(OTf)_3$ (10.0 mol%), DMAP (50.0 mol%), 4 Å MS (100 mg) and Cs_2CO_3 (0.1 mmol) in 1,4-dioxane (1.5 mL) was heated at 45 °C for 12 h; yields were determined by ^{1}H NMR using dibromomethane as an internal standard. [b] Concomitant product **3** and its yield.

ging the ester group in VDCP-diester **2** from an ethyl group to a methyl group or a benzyl group, the reaction took place smoothly, delivering the corresponding spiro-cyclohexadienones **4r** and **4s** in 27% and 50% yields, respectively. A *p*-QM with *t*-butyl replaced by i-propyl also underwent this reaction smoothly, giving the product **4t** in 50% yield. Meanwhile, the product **4u** with vinyl substitution at the alkene terminal position was also obtained in 44% yield.

Subsequently, a scale-up synthesis was performed with 1.0 mmol of substrate **1a** and 2.5 mmol of substrate **2a** under both conditions A and conditions B to verify the utility of the reaction, affording the corresponding products **3a** and **4a** in 58% and 60% yields, respectively (Scheme 4a). The catalytic asymmetric version of this divergent cycloaddition was also attempted (for details, see Schemes S3 and S4 in the ESI†), and we found that the use of chiral phosphine ligand (*R*)-SEGphos delivered **3y** in 64% yield with 25% ee value (Scheme 4b). In order to validate the reaction mechanism, we performed the following control experiments (Scheme 4c). The reactions of **1a** and **2a** were first allowed to proceed under standard conditions A without DPEphos as the ligand, affording the product **3a** in only 14% yield; only a trace amount of product **3a** was obtained in the absence of the Pd catalyst. These results indicate that the palladium catalyst and phosphorous ligand play critical roles in this reaction. In addition, under conditions B with Ph-PHOX as ligand, the yield decreased and the ratio of the two products did not change in the absence of DMAP or $Yb(OTf)_3$ as a Lewis acid, indicating that the Lewis acid and DMAP have no effect on the selectivity of the reaction.

In order to further understand the mechanistic details for these divergent palladium-catalyzed cycloadditions of VDCP-diesters with *p*-QMs, we conducted a series of DFT calculations to gain further insights. For the reaction with Ph-PHOX as the ligand, the DFT calculations were conducted at the SMD (solvent)/M06-D3/def2-tzvp/SDD//B3LYP(D3BJ)/6-31g(d,p)/SDD

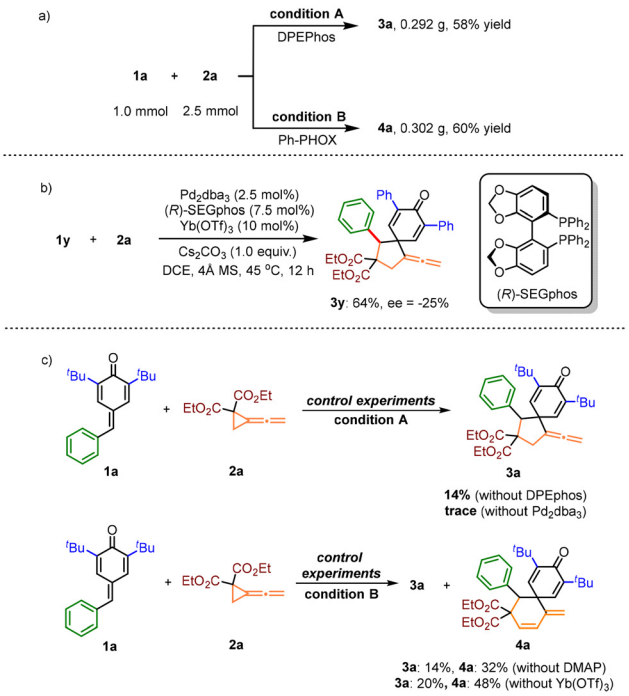

Scheme 4 (a) Scale-up reaction; (b) Asymmetric reaction of **1y**; (c) Control experiments.

level using the Gaussian 16 program.[12] The possible reaction pathways were investigated and are shown in Schemes 5 and 6 (for computational details, see the ESI†).

For the generation of product **3a** using DPEphos, we investigated the reaction pathway starting from a stable palladium complex **Int0** (shown in Scheme 5), in which the allene unit of **2a** is coordinated to the palladium catalyst combined with the DPEphos ligand. The complex **Int0** undergoes the ring-opening process to form the allenyl palladium intermediate **Int1** passing through transition state **TS1** with an energy barrier of 27.3 kcal mol^{-1}. Another possible zwitterionic π-propargyl palladium intermediate **Int1′** was also investigated; however, the energy of **Int1′** is higher than that of **Int1** by 8.2 kcal mol^{-1}; the complex **Int0** has to overcome an energy barrier of 31.6 kcal mol^{-1} through transition state **TS1′** to obtain zwitterionic π-propargyl palladium **Int1′**. Thus, the formation of allenyl palladium intermediate **Int1** is more favourable thermodynamically and kinetically. Next, the intermediate **Int1** is associated to the alkene moiety of the *p*-QM to afford an intermediate **Int2**, which is an exothermic process (ΔG = −3.9 kcal mol^{-1}). The nucleophilic attack at the C1 position of **1a** generates the intermediate **Int3″** *via* **TS2** with an energy barrier of 24.6 kcal mol^{-1}. Isomerization of **Int3″** to zwitterionic π-propargyl palladium intermediate **Int3** is exothermic by 14.8 kcal mol^{-1}, where the carbon anion of **Int3** selectively attacks the internal carbon atom C5 of the Pd-π-propargyl unit *via* **TS4** to afford the complex **Int4** of the Pd(0) catalyst with the [3 + 2] cycloaddition product. The energy barrier for [3 + 2] cycloaddition is 2.8 kcal mol^{-1}, which is much lower than that of the competitive pathway involving attacking the Pd-π-propargyl unit at its central carbon C4 to generate the corresponding pallada-cyclobutene intermediate **Int4″** (17.5 kcal mol^{-1} *via* **TS3″**), which is the key intermediate for generation of the [4 + 2] cycloaddition product **4a**. This calculation result indicates that the formation of the [3 + 2] cycloaddition product is favorable thermodynamically and kinetically; this is also consistent with the fact that we only obtained product **3a** in experiments using DPEphos as the ligand. Subsequently,

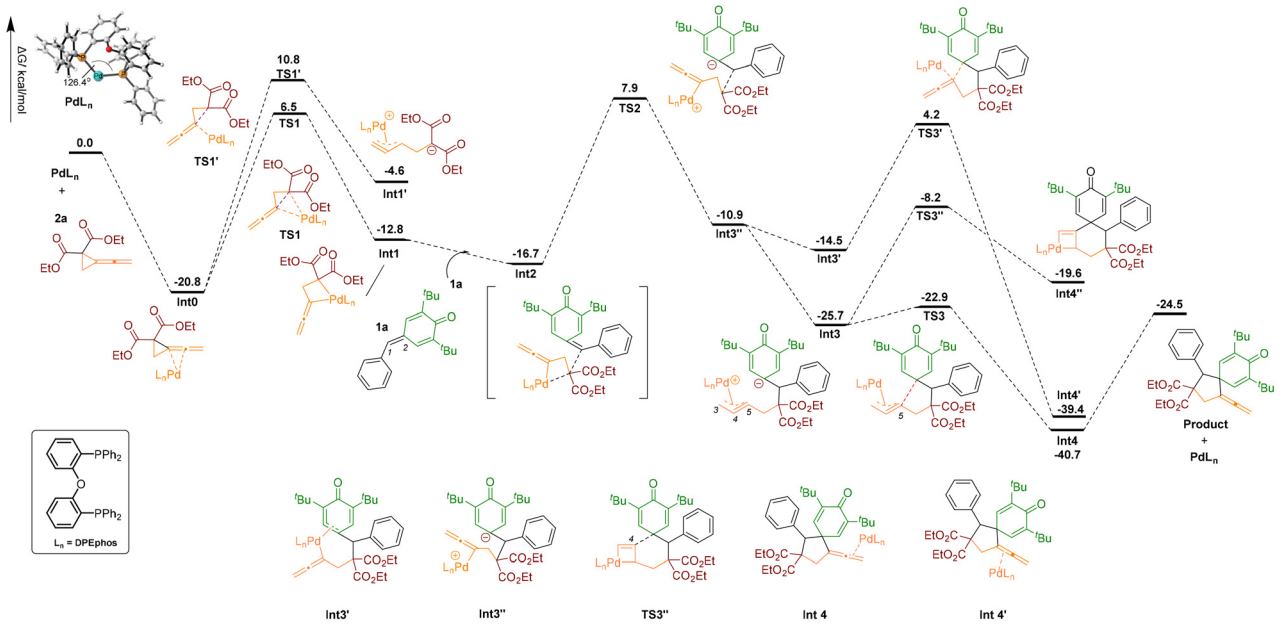

Scheme 5 DFT calculations on the possible reaction pathways under conditions A.

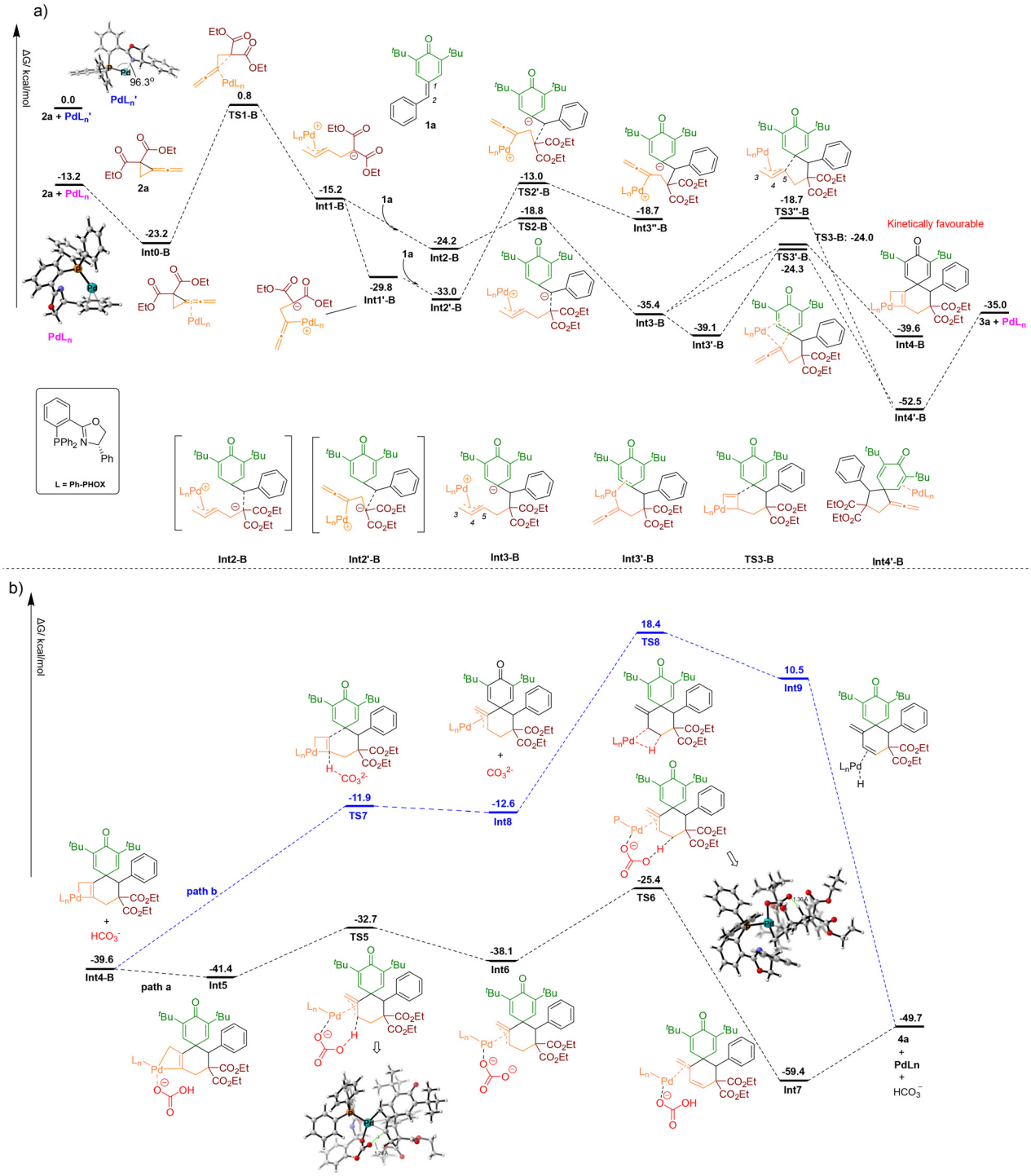

Scheme 6 (a) DFT calculations on the possible reaction pathways under conditions B; (b) DFT calculations on the proton transfer process assisted by base.

another possible isomerization intermediate **Int3′**, in which both the allyl of **1a** and the allene unit are coordinated to the palladium catalyst, is also investigated. However, the intermediate **Int3′** undergoes the ring-closing step to produce an intermediate **Int4″** *via* transition state **TS3′**, this energy barrier of 18.7 kcal mol^{-1} is higher than the competitive pathway passing through transition state **TS3**, therefore, this pathway is ruled out. Finally the intermediate **Int4** dissociates to the final product **3a** and the catalyst is regenerated.

We also investigated the reaction pathway for conditions B, in which Ph-PHOX is utilized as the ligand (shown in Scheme 6a).[13] It should be mentioned here that the stabilized

structure of Ph-PHOX-Pd(0) involves palladium coordinated to the phosphorus atom and benzene ring of the ligand (**PdL$_n$**). The energy of **PdL$_n$** is lower than that of the Ph-PHOX-Pd(0) catalyst (**PdL$_n$′**) by 13.2 kcal mol^{-1}, in which palladium is coordinated to the ligand's phosphorus atom and nitrogen atom; this result may be due to the hemilability of Ph-PHOX. The coordination angle of Ph-PHOX with palladium (**PdL$_n$′**) is only 96.3°, which is much smaller than the angle of 126.4° for DPEphos, and may affect the site of attack in the ring closure step. Next, a stable palladium complex **Int0-B**, in which allene units of **2a** are coordinated to Ph-PHOX-Pd(0), is generated. **Int0-B** can undergo an oxidative ring cleavage reaction to give a zwitterionic π-propargyl palladium intermediate **Int1-B** through **TS1-B** with an energy barrier of 24.0 kcal mol^{-1}. Subsequently, the palladium intermediate **Int1-B** is associated to **1a** to form a complex **Int2-B**. Alternatively, the zwitterionic π-propargyl palladium intermediate **Int1-B** is isomerized to another intermediate **Int1′-B** due to a different coordination mode, which is an exothermic process (ΔG = −14.6 kcal mol^{-1}). Passing through transition state **TS2-B** with an energy barrier of 5.4 kcal mol^{-1}, the intermediate **Int3-B** is formed in an exothermic process (ΔG = −11.2 kcal mol^{-1}). Although the energies of **Int1′-B** and **Int2′-B** are lower than those of **Int1-B** and **Int2-B**, respectively, a higher energy barrier of 20.0 kcal mol^{-1} has to be overcome to access the intermediate **Int3′-B** in a highly endothermic process (ΔG = 14.3 kcal mol^{-1}). Thus, the formation of intermediate **Int3-B** is thermodynamically and kinetically favorable. Next, the pathway with the lower energy barrier of 11.4 kcal mol^{-1} *via* **TS3-B** in the next process involves the carbon anion of **Int3-B** attacking the Pd-π-propargyl unit at its central carbon C4 to generate the pallada-cyclobutene intermediate **Int4-B**, which is the key intermediate for generation of the [4 + 2] product **4a**. Another competitive path involving the carbon anion of **Int3-B** attacking the internal carbon atom C5 of the Pd-π-propargyl unit has an energy barrier of 16.7 kcal mol^{-1} *via* **TS3″-B** to give an intermediate **Int4′-B**, which further dissociates to the [3 + 2] product **3a** and palladium catalyst. Another possible isomerization intermediate **Int3′-B** passing through transition state **TS3′-B** with an energy barrier of 14.8 kcal mol^{-1} also can generate intermediate **Int4′-B**; however, the barrier is still higher than that for generation of intermediate **Int4-B**. These calculation results show that the formation of intermediate **Int4-B** is the most kinetically favorable, indicating the generation of the [4 + 2] product **4a** is kinetically favorable. These results may account for why product **4a** is mainly obtained under reaction conditions B.

Next, we continued to investigate the following reaction steps involving the proton transfer assisted by base from intermediate **Int4** (Scheme 6b).[14] At this stage, two alternative pathways are investigated, respectively. One of them is **path a** involving the base coordinated to the palladium and the other is **path b** involving the direct proton transfer and no coordination between the base and the palladium. As depicted in **path a**, the bicarbonate, which is generated by trace amounts of water in the system and the base, is coordinated to **Int4-B**, affording the intermediate **Int5** in a process that is exothermic by 1.8 kcal mol^{-1}, due to the hemilability of the ligand, wherein bicarbonate undergoes ligand exchange with the nitrogen atom in the ligand. The generated intermediate **Int5** then protonates the allyl alpha position *via* transition state **TS5** to form **Int6** with a small energy barrier of 8.7 kcal mol^{-1}. The hydrogen in the allylic β-site of **Int6** then approaches the undissociated carbonate to undergo β-hydrogen elimination *via* **TS6** with an energy barrier of 12.7 kcal mol^{-1}. Finally, the product complex **Int7** dissociates to give the [4 + 2] product **4a** in a 9.7 kcal mol^{-1} endothermic process. In contrast, due to the higher energy barrier of 27.7 kcal mol^{-1} for direct proton transfer by bicarbonate and the large ring tension of the four-membered ring transition state **TS8** during β-hydrogen elimination, the reaction mechanism *via* **path b** is energetically unfavorable, and is excluded.

On the basis of DFT calculation results and the previously reported processes, a plausible mechanism for the [3 + 2] and [4 + 2] cycloadditions is depicted in Scheme 7. Pd(0) complex **I** and VDCP-diester **2a** undergo an oxidative addition and generate the zwitterionic Pd species **II** or **II′**. The nucleophilic carbon anion of intermediate **II** or **II′** attacks **1a** to afford an intermediate **III**. Then the carbon anion selectively attacks the inner carbon atom to generate the corresponding five-membered [3 + 2] cycloaddition product **3a** *via* transition state **VI′** and simultaneously regenerate the catalyst Pd(0) with DPEphos with a large bite angle. On the other hand, when using Ph-PHOX as a small bite angle ligand, the carbon anion selectively attacks the central carbon of the allene moiety to generate pallada-cyclobutene intermediate **IV**, then **IV** undergoes base-induced protonation and β-hydride elimination to obtain the six-membered [4 + 2] cycloaddition product **4a** and

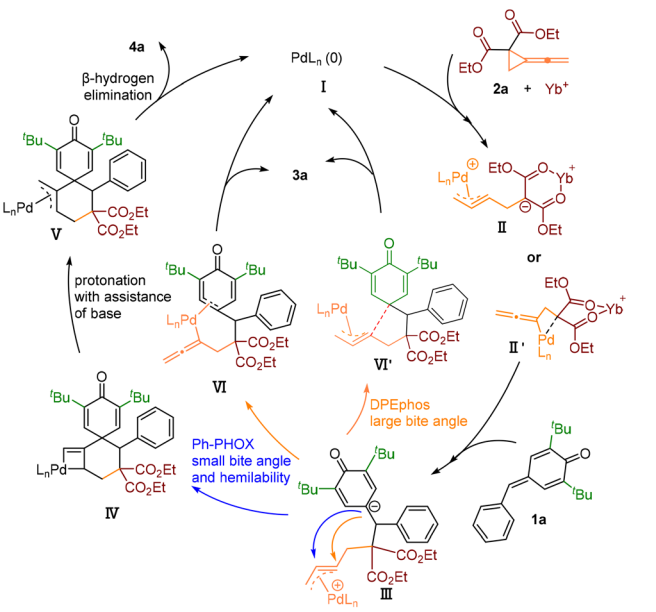

Scheme 7 The plausible mechanism of the palladium-catalyzed cycloaddition reactions.

regenerate the Pd(0) catalyst; simultaneously product **3a** was obtained through intermediate **VI**. Additives and bases play auxiliary roles in this reaction. $Yb(OTf)_3$ as a Lewis acid additive probably promotes the C–C bond cleavage of the cyclopropane ring through coordination with the ester moieties;[15] 4 Å MS as an additive get rid of the ambient moisture; DMAP and Cs_2CO_3 as base additives probably stabilize the zwitterionic palladium species and assist the proton transfer process.

Conclusions

In summary, a regioselective divergent cycloaddition of *p*-QMs with zwitterionic palladium intermediates generated from VDCP-diesters has been developed, and two different types of spiro-cyclohexadienone products, namely [3 + 2] and [4 + 2] cycloaddition products, can be synthesized by switching ligands in good to excellent total yields with good functional group compatibility. DFT calculations reveal that the [3 + 2] cycloaddition product is favorable thermodynamically and kinetically using DPEphos as a ligand, probably due to the large bite angle of DPEphos which makes the [3 + 2] cycloaddition mode preferred. The hemilability and the small bite angle of Ph-PHOX probably lead to the key [4 + 2] cycloaddition intermediate being kinetically favourable; thus, the [4 + 2] cycloaddition product was mainly obtained in experiments. Our group will further develop highly enantioselective cycloadditions of VDCPs with *p*-QMs catalyzed by palladium in the future and apply this reaction to the synthesis of biologically active molecules.

Author contributions

Yong-Jie Long discovered the reactions. Min Shi and Yong-Jie Long designed the experiments. Jia-Hao Shen performed the experiments and analysed the results. Min Shi, Yin Wei and Jia-Hao Shen wrote the manuscript. Yin Wei and Jia-Hao Shen performed and described the computational section.

Conflicts of interest

There are no conflicts to declare.

Acknowledgements

We are grateful for the financial support from the National Key R & D Program of China (2023YFA1506700), the National Natural Science Foundation of China (21372250, 21121062, 21302203, 21772037, 21772226, 21861132014, 91956115 and 22171078) and the Fundamental Research Funds for the Central Universities 222201717003.

References

1 (*a*) L. K. Smith and I. R. Baxendale, Total syntheses of natural products containing spirocarbocycles, *Org. Biomol. Chem.*, 2015, **13**, 9907–9933; (*b*) R. Chen, S. Jia, Y. Man, H.-G. Cheng and Q. Zhou, A Concise Total Synthesis of (±)-Stepharine and (±)-Pronuciferine, *Synthesis*, 2023, DOI: 10.1055/a-1984-0755; (*c*) G. Blay, L. Cardona, A. M. Collado, B. García, V. Morcillo and J. R. Pedro, Synthesis of Spirovetivane Sesquiterpenes from Santonin. Synthesis of (+)-Anhydro-β-rotunol and All Diastereomers of 6,11-Spirovetivadiene, *J. Org. Chem.*, 2004, **69**, 7294–7302; (*d*) C.-P. Chung, C.-Y. Hsu, J.-H. Lin, Y.-H. Kuo, W. Chiang and Y.-L. Lin, Antiproliferative Lactams and Spiroenone from Adlay Bran in Human Breast Cancer Cell Lines, *J. Agric. Food Chem.*, 2011, **59**, 1185–1194; (*e*) A. R. Díaz-Marrero, G. Porras, Z. Aragón, J. M. de la Rosa, E. Dorta, M. Cueto, L. D'Croz, J. Maté and J. Darias, Carijodienone from the Octocoral Carijoa multiflora. A Spiropregnane-Based Steroid, *J. Nat. Prod.*, 2011, **74**, 292–295; (*f*) A. B. Petersen, M. H. Rønnest, T. O. Larsen and M. H. Clausen, The Chemistry of Griseofulvin, *Chem. Rev.*, 2014, **114**, 12088–12107; (*g*) W. Li, X. Xu, P. Zhang and P. Li, Recent Advances in the Catalytic Enantioselective Reactions of *para*-Quinone Methides, *Chem. – Asian J.*, 2018, **13**, 2350–2359.

2 (*a*) X. Liu, Y. Ren, L. Zhu, T. Li, W. Xu, Y. Liu, K.-W. Tang and B. Xiong, Recent advances in the cyclization of *para*-quinone methides, *Tetrahedron*, 2023, **148**, 133655; (*b*) W. Baik, H. J. Lee, J. M. Jang, S. Koo and B. H. Kim, NBS-Promoted Reactions of Symmetrically Hindered Methylphenols via *p*-Benzoquinone Methide, *J. Org. Chem.*, 2000, **65**, 108–115; (*c*) W. R. Hatchard, Syntheses by Free-radical Reactions. VII. The Reaction of 2,6-Di-t-butyl-4-methylphenol and 2,6-Di-t-butyl-4-isopropylphenol with Chloroprene, *J. Am. Chem. Soc.*, 1958, **80**, 3640–3642; (*d*) J. D. McClure, Synthesis of Spiroundecatrienones from 2,6-Di-t-butylquinone Methide and Butadienes, *J. Org. Chem.*, 1962, **27**, 2365–2368.

3 (*a*) R. Pan, L. Hu, C. Han, A. Lin and H. Yao, Cascade Radical 1,6-Addition/Cyclization of *para*-Quinone Methides: Leading to Spiro[4.5]deca-6,9-dien-8-ones, *Org. Lett.*, 2018, **20**, 1974–1977; (*b*) X.-Z. Zhang, Y.-H. Deng, K.-J. Gan, X. Yan, K.-Y. Yu, F.-X. Wang and C.-A. Fan, Tandem Spirocyclopropanation/Rearrangement Reaction of Vinyl *p*-Quinone Methides with Sulfonium Salts: Synthesis of Spirocyclopentenyl *p*-Dienones, *Org. Lett.*, 2017, **19**, 1752–1755; (*c*) B. Debnath, T. Sarkar, P. Karjee, S. K. Purkayastha, A. K. Guha and T. Punniyamurthy, Palladium-Catalyzed Annulative Coupling of Spirovinylcyclopropyl Oxindoles with *p*-Quinone Methides, *J. Org. Chem.*, 2023, **88**, 9704–9719.

4 (*a*) W.-D. Chu, L.-F. Zhang, X. Bao, X.-H. Zhao, C. Zeng, J.-Y. Du, G.-B. Zhang, F.-X. Wang, X.-Y. Ma and C.-A. Fan, Asymmetric Catalytic 1,6-Conjugate Addition/Aromatization of *para*-Quinone Methides: Enantioselective Introduction of Functionalized Diarylmethine Stereogenic Centers,

Angew. Chem., Int. Ed., 2013, **52**, 9229–9233; (*b*) K. Zhao, Y. Zhi, A. Wang and D. Enders, Asymmetric Organocatalytic Synthesis of 3-Diarylmethine-Substituted Oxindoles Bearing a Quaternary Stereocenter via 1,6-Conjugate Addition to *para*-Quinone Methides, *ACS Catal.*, 2016, **6**, 657–660; (*c*) P. Goswami, S. Sharma, G. Singh and R. V. Anand, Bis(amino)cyclopropenylidene Catalyzed Rauhut–Currier Reaction between α,β-Unsaturated Carbonyl Compounds and *para*-Quinone Methides, *J. Org. Chem.*, 2018, **83**, 4213–4220; (*d*) X.-Z. Zhang, Y.-H. Deng, X. Yan, K.-Y. Yu, F.-X. Wang, X.-Y. Ma and C.-A. Fan, Diastereoselective and Enantioselective Synthesis of Unsymmetric β,β-Diaryl-α-Amino Acid Esters via Organocatalytic 1,6-Conjugate Addition of *para*-Quinone Methides, *J. Org. Chem.*, 2016, **81**, 5655–5662; (*e*) F.-S. He, J.-H. Jin, Z.-T. Yang, X. Yu, J. S. Fossey and W.-P. Deng, Direct Asymmetric Synthesis of β-Bis-Aryl-α-Amino Acid Esters via Enantioselective Copper-Catalyzed Addition of *p*-Quinone Methides, *ACS Catal.*, 2016, **6**, 652–656.

5 Three-membered ring: (*a*) S. B. Kale, P. K. Jori, T. Thatikonda, R. G. Gonnade and U. Das, 1,6-Conjugate-Addition-Induced [2 + 1] Annulation of *para*-Quinone Methides and Pyrazolones: Synthesis of Bis-Spiro Compounds with Contiguous Quaternary Spiro-Centers, *Org. Lett.*, 2019, **21**, 7736–7740; (*b*) Z. Yuan, X. Fang, X. Li, J. Wu, H. Yao and A. Lin, 1,6-Conjugated Addition-Mediated [2 + 1] Annulation: Approach to Spiro[2.5]octa-4,7-dien-6-one, *J. Org. Chem.*, 2015, **80**, 11123–11130; (*c*) L. Roiser and M. Waser, Enantioselective Spirocyclopropanation of *para*-Quinone Methides Using Ammonium Ylides, *Org. Lett.*, 2017, **19**, 2338–2341; (*d*) Y.-H. Deng, W.-D. Chu, Y.-H. Shang, K.-Y. Yu, Z.-L. Jia and C.-A. Fan, $P(NMe_2)_3$-Mediated Umpolung Spirocyclopropanation Reaction of *p*-Quinone Methides: Diastereoselective Synthesis of Spirocyclopropane-Cyclohexadienones, *Org. Lett.*, 2020, **22**, 8376–8381; (*e*) X.-Z. Zhang, J.-Y. Du, Y.-H. Deng, W.-D. Chu, X. Yan, K.-Y. Yu and C.-A. Fan, Spirocyclopropanation Reaction of *para*-Quinone Methides with Sulfonium Salts: The Synthesis of Spirocyclopropanyl *para*-Dienones, *J. Org. Chem.*, 2016, **81**, 2598–2606; (*f*) K. Gai, X. Fang, X. Li, J. Xu, X. Wu, A. Lin and H. Yao, Synthesis of spiro[2.5]octa-4,7-dien-6-one with consecutive quaternary centers via 1,6-conjugate addition induced dearomatization of *para* -quinone methides, *Chem. Commun.*, 2015, **51**, 15831–15834; (*g*) J.-R. Zhang, H.-S. Jin, J. Sun, J. Wang and L.-M. Zhao, Time-Economical Synthesis of Bis-Spiro Cyclopro-panes via Cascade 1,6-Conjugate Addition/Dearomatization Reaction of *para*-Quinone Methides with 3-Chlorooxindoles, *Eur. J. Org. Chem.*, 2020, 4988–4994.

6 Five-membered ring: (*a*) Y. Su, Y. Zhao, B. Chang, X. Zhao, R. Zhang, X. Liu, D. Huang, K.-H. Wang, C. Huo and Y. Hu, [3 + 2] Cycloaddition of *para*-Quinone Methides with Nitrile Imines: Approach to Spiro-pyrazoline-cyclohexadienones, *J. Org. Chem.*, 2019, **84**, 6719–6728; (*b*) M. Soleymani and S. Jahanparvar, A computational study on the [3 + 2] cycloaddition of *para*-quinone methides with nitrile imines: a two-stage one-step mechanism, *Monatsh. Chem.*, 2020, **151**, 51–61; (*c*) Z. Yuan, W. Wei, A. Lin and H. Yao, Bifunctional Organo/Metal Cooperatively Catalyzed [3 + 2] Annulation of *para*-Quinone Methides with Vinylcyclopropanes: Approach to Spiro[4.5]deca-6,9-diene-8-ones, *Org. Lett.*, 2016, **18**, 3370–3373; (*d*) L. Roiser, K. Zielke and M. Waser, Formal (4 + 1) Cyclization of Ammonium Ylides with Vinylogous *para*-Quinone Methides, *Synthesis*, 2018, **50**, 4047–4054; (*e*) G.-T. Song, Y. Liu, X.-Y. Hu, S.-T. Li, J.-B. Liu, Y. Li and C.-H. Qu, Microwave-assisted copper catalyzed decarboxylative reductive coupling of *para*-quinone methides with 3-indoleacetic acids: rapid access to polycyclic spiroindole-quinone derivatives, *Org. Chem. Front.*, 2023, **10**, 1512–1520; (*f*) Z.-L. Jia, X.-T. An, Y.-H. Deng, H.-B. Wang, K.-J. Gan, J. Zhang, X.-H. Zhao and C.-A. Fan, Palladium-Catalyzed Asymmetric (2 + 3) Annulation of *p*-Quinone Methides with Trimethyleneme-thanes: Enantioselective Synthesis of Functionalized Chiral Spirocyclopentyl *p*-Dienones, *Org. Lett.*, 2020, **22**, 4171–4175; (*g*) Z. Yuan, L. Liu, R. Pan, H. Yao and A. Lin, Silver-Catalyzed Cascade 1,6-Addition/Cyclization of *para*-Quinone Methides with Propargyl Malonates: An Approach to Spiro[4.5]deca-6,9-dien-8-ones, *J. Org. Chem.*, 2017, **82**, 8743–8751; (*h*) C. Ma, Y. Huang and Y. Zhao, Stereoselective 1,6-Conjugate Addition/Annulation of *para*-Quinone Methides with Vinyl Epoxides/Cyclopropanes, *ACS Catal.*, 2016, **6**, 6408–6412.

7 Six-membered ring: (*a*) G. S. Ghotekar, S. R. Shirsath, A. C. Shaikh and M. Muthukrishnan, 1,6-Conjugate addition initiated formal [4 + 2] annulation of *p*-quinone methides with sulfonyl allenols: a unique access to spiro [5.5]undeca-1,4-dien-3-one scaffolds, *Chem. Commun.*, 2020, **56**, 5022–5025; (*b*) Z.-L. Jia, X.-T. An, Y.-H. Deng, L.-H. Pang, C.-F. Liu, L.-L. Meng, J.-K. Xue, X.-H. Zhao and C.-A. Fan, Palladium-Catalyzed Asymmetric (4 + 2) Annulation of γ-Methylidene-δ-valerolactones with Alkenes: Enantioselective Synthesis of Functionalized Chiral Cyclohexyl Spirooxindoles, *Org. Lett.*, 2021, **23**, 745–750; (*c*) Z. Yuan, R. Pan, H. Zhang, L. Liu, A. Lin and H. Yao, Palladium-catalyzed Oxa-[4 + 2] Annulation of *para*-Quinone Methides, *Adv. Synth. Catal.*, 2017, **359**, 4244–4249; (*d*) L. Cao, F. Hu, J. Dong, X.-M. Zhang and S.-S. Li, Aromatization-driven cascade [1,5]-hydride transfer/cyclization for synthesis of spirochromanes, *Org. Chem. Front.*, 2023, **10**, 1796–1802; (*e*) R. A. Gaikwad, A. T. Savekar and S. B. Waghmode, Metal-Free Approach for Oxa-spirocyclohexadienones through [3 + 2]/[4 + 2] ipso-Cyclization of *para*-Quinone Methides with Halo Alcohols, *J. Org. Chem.*, 2023, **88**, 9987–10001.

8 (*a*) B. Niu, Y. Wei and M. Shi, Recent advances in annulation reactions based on zwitterionic π-allyl palladium and propargyl palladium complexes, *Org. Chem. Front.*, 2021, **8**, 3475–3501; (*b*) J. Du, Y.-F. Li and C.-H. Ding, Recent advances of Pd-π-allyl zwitterions in cycloaddition reactions, *Chin. Chem. Lett.*, 2023, **34**, 108401; (*c*) Z. Han, Y. Xue, X. Li, X. Hu, X.-Q. Dong, J. Sun and H. Huang,

Studies on the [4 + 2] cycloaddition and allylic substitution of indole-fused zwitterionic π-allylpalladium, *Org. Biomol. Chem.*, 2023, **21**, 8162–8169.

9 (*a*) A. E. Nibbs, T. D. Montgomery, Y. Zhu and V. H. Rawal, Access to Spirocyclized Oxindoles and Indolenines via Palladium-Catalyzed Cascade Reactions of Propargyl Carbonates with 2-Oxotryptamines and Tryptamines, *J. Org. Chem.*, 2015, **80**, 4928–4941; (*b*) Z. Yang, B. Zhang, Y. Long and M. Shi, Palladium-catalyzed hydroamination of vinylidenecyclopropane-diester with pyrroles and indoles: an approach to azaaromatic vinylcyclopropanes, *Chem. Commun.*, 2022, **58**, 9926–9929; (*c*) R.-D. Gao, C. Liu, L.-X. Dai, W. Zhang and S.-L. You, Pd(0)-Catalyzed Alkenylation and Allylic Dearomatization Reactions between Nucleophile-Bearing Indoles and Propargyl Carbonate, *Org. Lett.*, 2014, **16**, 3919–3921; (*d*) A. Iwata, S. Inuki, S. Oishi, N. Fujii and H. Ohno, Synthesis of fused tetracyclic spiroindoles via palladium-catalysed cascade cyclisation, *Chem. Commun.*, 2013, **50**, 298–300.

10 (*a*) Z. Meng, J. Yan, C. Ning, M. Shi and Y. Wei, Construction of pyrroles, furans and thiophenes via intramolecular cascade desulfonylative/dehydrogenative cyclization of vinylidenecycl-opropanes induced by NXS (X = I or Br), *Chem. Sci.*, 2023, **14**, 7648–7655; (*b*) S. Yang and M. Shi, Recent Advances in Transition-Metal-Catalyzed/Mediated Transformations of Vinylidenecyclopropanes, *Acc. Chem. Res.*, 2018, **51**, 1667–1680; (*c*) Z. Meng, X. Zhang and M. Shi, Visible-light mediated cascade cyclization of ene-vinylidenecyclopropanes: access to fluorinated heterocyclic compounds, *Org. Chem. Front.*, 2021, **8**, 3796–3801.

11 B. Niu, Y. Wei and M. Shi, Palladium catalyzed divergent cycloadditions of vinylidenecyclopropane-diesters with methyleneindolinones enabled by zwitterionic π-propargyl palladium species, *Chem. Commun.*, 2021, **57**, 4783–4786.

12 M. J. Frisch, G. W. Trucks, H. B. Schlegel, G. E. Scuseria, M. A. Robb, J. R. Cheeseman, G. Scalmani, V. Barone, G. A. Petersson, H. Nakatsuji, X. Li, M. Caricato, A. V. Marenich, J. Bloino, B. G. Janesko, R. Gomperts, B. Mennucci, H. P. Hratchian, J. V. Ortiz, A. F. Izmaylov, J. L. Sonnenberg, D. Williams-Young, F. Ding, F. Lipparini, F. Egidi, J. Goings, B. Peng, A. Petrone, T. Henderson, D. Ranasinghe, V. G. Zakrzewski, J. Gao, N. Rega, G. Zheng, W. Liang, M. Hada, M. Ehara, K. Toyota, R. Fukuda, J. Hasegawa, M. Ishida, T. Nakajima, Y. Honda, O. Kitao, H. Nakai, T. Vreven, K. Throssell, J. A. Montgomery Jr., J. E. Peralta, F. Ogliaro, M. J. Bearpark, J. J. Heyd, E. N. Brothers, K. N. Kudin, V. N. Staroverov, T. A. Keith, R. Kobayashi, J. Normand, K. Raghavachari, A. P. Rendell, J. C. Burant, S. S. Iyengar, J. Tomasi, M. Cossi, J. M. Millam, M. Klene, C. Adamo, R. Cammi, J. W. Ochterski, R. L. Martin, K. Morokuma, O. Farkas, J. B. Foresman and D. J. Fox, *Gaussian 16, Revision C.01*, Gaussian, Inc., Wallingford CT, 2016.

13 C. Y. Legault, *CYLview, 1.0b*, Université de Sherbrooke, 2009 (**https://www.cylview.org**).

14 G. Zhang, Y.-K. Song, F. Zhang, Z.-J. Xue, M.-Y. Li, G.-S. Zhang, B.-B. Zhu, J. Wei, C. Li, C.-G. Feng and G.-Q. Lin, Palladium-catalyzed allene synthesis enabled by β-hydrogen elimination from sp^2-carbon, *Nat. Commun.*, 2021, **12**, 728.

15 L. Wu and M. Shi, Ring-Opening Reaction of Vinylidenecyclopropanediesters Catalyzed by $Re_2(CO)_{10}$ or $Yb(OTf)_3$, *Eur. J. Org. Chem.*, 2011, 1099–1105.